Supplementary Information

Determining the Cytosolic Stability of Small DNA Nanostructures *in Cellula*

Divita Mathur,[1,2]* Katherine E. Rogers,[2,3] Sebastián A. Díaz,[2] Megan E. Muroski,[2,4] William P. Klein,[2,5] Okhil K. Nag,[2] Kwahun Lee,[2,4] Lauren D. Field,[2,5] James B. Delehanty,[2] and Igor L. Medintz[2]*

[1]College of Science, George Mason University, Fairfax, VA 22030 USA.

[2]Center for Bio/Molecular Science and Engineering Code 6900, US Naval Research Laboratory, Washington, DC 20375 USA.

[3]Fischell Department of Bioengineering, University of Maryland, College Park, MD 20742 USA.

[4]American Society of Engineering Education, Washington, DC 20036 USA.

[5]National Research Council, Washington, DC 20001 USA.

*Corresponding authors: igor.medintz@nrl.navy.mil, dmathur4@gmu.edu

Table of Contents

Section I: Experimental Methods

Materials.

Dye-modified and unlabeled DNA oligonucleotides were obtained from Integrated DNA Technologies (Coralville, IA) in lyophilized form and reconstituted in molecular biology grade water to a stock concentration of 100 μM. HEPES (4-(2-hydroxyethyl)-1-piperazineethanesulfonic acid) buffer, magnesium chloride $MgCl_2$, molecular biology grade water, and aurintricarboxylic acid (ATA) were obtained from Sigma-Aldrich. Centrifuge (Amicon) filters were obtained from Milipore. Nuclease enzymes (DNase I M0303L, ExoI M0293L, ExoIII M0206L) were obtained from New England Biolabs.

DNA Nanostructure Assembly.

DNA crosshairs and tetrahedron were all prepared using the same procedure. Equimolar concentrations of constituent oligonucleotides were combined in 50 mM HEPES 5 mM $MgCl_2$ pH 9 (HEPES+Mg buffer). DNA crosshairs and tetrahedron were prepared at final concentrations of 1.5 and 1 μM, respectively. Annealing procedure was as follows: 85 ºC to 4 ºC at the rate of 2 min/ºC with storage at 4 ºC. Crosshairs underwent size-exclusion purification using Amicon centrifugation columns at a molecular weight cutoff of 50 kDa. Amicon filters were rinsed with 450 μL HEPES+Mg buffer, spun down at 12000×*g* for 1 min. 100-400 μL of crosshair sample was added and spun down at 9000×*g* for 3 min. 300 μL of buffer was added to the filter and spun down three times at 9000×*g* for 3 min. Sample was recovered by inverting the column into a clean 2 mL vial and spun down at 2000×*g* for 3 min. Sample concentration was measured at 260 nm with a UV-vis spectrophotometer. Both samples were prepared at a 1 μM final concentration. The octacross was prepared at a final concentration of 0.5 μM.

Steady State Absorption, Fluorescence Measurements, and Nuclease Assays.

Steady-state absorption spectra were measured using 120 μL of each sample in a 10 mm path length cuvette with an Agilent 8453 diode array UV–vis spectrophotometer. Excitation and emission spectra were measured using 75 μL of each sample loaded into a Corning black flat-bottom 96-well plate in a multifunction microtiter plate reader (Tecan Spark) with excitation at 466 nm. The enzyme activity plate assay was performed using a Corning black flat-bottom 384-

well plate and the kinetic loop function in the plate reader. The excitation and emission spectra were corrected for wavelength dependent instrumental effects. Data analysis and graphical representation of the data was performed on Origin 2020.

Cell Culture.

COS-1 cells (monkey kidney epithelial cells, ATCC CRL-1650) were cultured in growth medium (Gibco's Dulbecco's Modified Eagle's Medium (DMEM) from Thermo Fisher Scientific was supplemented with 10% fetal bovine serum (FBS) and 1% antibiotic-antimycotic). Primary human dermal fibroblast cells were obtained from Lonza and were cultured in DMEM with 10% FBS and 1% antibiotic-antimycotic. A549 cells (ATCC CCL-185) were cultured in F-12K Medium (ATTC, cat. 30-2004) added with 10% FBS and 1% antibiotic-antimycotic. HeLa cells (ATCC CCL-2) were grown using Minimum Essential Medium (MEM) with 10% FBS and 1% antibiotic-antimycotic. Finally, normal human astrocytes (Creative Biolabs) were cultured using an Astrocyte Growth Medium kit provided by the same company and plated on poly-L-lysine coated glass plates in preparation for microinjection. All cells were maintained at 37ºC in a humidified atmosphere consisting of 5% CO_2 and were subcultured according to manufacturer protocols in T-75 cell culture flasks. Two days before use in microinjection experiments, cells were plated on a 35 mm MatTek dish (MatTek, USA) with 3 mL native media. Medium was changed 24 h before microinjection.

Live cell confocal microscopy.

Live cell imaging was performed using differential interference contrast and confocal laser scanning microscopy using a Nikon Eclipse Ti2 confocal inverted microscope (Nikon Instruments, USA) using laser lines at 488 nm, 561 nm, and 640 nm. All data was collected with a Plan Apo 60X oil objective (NA 1.4). Live cell imaging solution (3 mL, Life Technologies) was added to cells before imaging. **Table S7** summarizes the various channels that were measured. Images were acquired and fluorescence intensity was analyzed using NIS Elements Imaging Software, Version 5.21.02.

Live cell microinjection.

10 μL of DNA nanostructure solution was loaded into Eppendorf Femtotip microinjection needles; microinjection into cells was performed using an Eppendorf microinjector 4i manipulator. Injection time (0.3 s) and pressure (500 hPa), and 45 hPa compensation pressure, provided *via* an Eppendorf Femtojet 4i, was used to maintain consistently injected volumes across experiments. Each cell was injected within 1 minute before beginning image capture.

Statistical analysis.

To determine the sample size required to make a statistically informed decision about the behavior of the DNA structures inside the cells, we calculated that a sample size of > 16 cells per group would be sufficient to detect a 40% difference between the means of groups (variance 40%) with 80% statistical power (derived from open-sourced tools). Moreover, previously published results using cell microinjections have used 10 to 600 cells depending on manual or automated injection procedures.[1, 2] In this work, 10-20 cells per experiment were injected which was reproduced 3-5 times to acquire a total of 60-90 cells per sample (**Table S6**). In each sample the standard deviation from the average is reported.

Section II: DNA sequences for each structure

Table S1: DNA nanocrosshair and octacrosshair sequences.

Name	**Sequence (5' to 3')**	Modification	Length (nt)
Core1	CTTGTCGGGTTCAGCCGCAATCTTCGCCTGCACTCTACC	n/a	39
Core2	CTTGTCGGGTAGAGTGCAGGCGATGAGCACGAGTCTTGC	n/a	39
Core3	CTTGTCGGCAAGACTCGTGCTCACCGAATGCCACCACGC	n/a	39
NC-Core4	CTTGTCGGCGTGGTGGCATTCGGAGATTGCGGCTGAACC	n/a	39
OC-Core4	CTTGTCGGCGTGGTGGCATTCGGCGTCCAGCTCTGATCC	n/a	39
OC-Core5	CTTGTCGGGATCAGAGCTGGACGACAATGACGTAGGTCC	n/a	39
OC-Core6	CTTGTCGGGACCTACGTCATTGTACTATGGCACACATCC	n/a	39
OC-Core7	CTTGTCGGGATGTGTGCCATAGTGGTCAACGCATACACC	n/a	39
OC-Core8	CTTGTCGGGTGTATGCGTTGACCAGATTGCGGCTGAACC	n/a	39
AF488_UN	CGACAAGTAAGCCCA	n/a	15
AT550_UN	ATCCATCATTGGGCTTA	n/a	17
AT633_UN	ATGATGGAT	n/a	9
AF488	/5Alex488N/CGACAAGTAAGCCCA	AF488	15
AT550	ATCCATCATTGGGCTTA-AT550	AT550	17
AT633	AT633-ATGATGGAT	AT633	9

Table S2: DNA tetrahedron sequences.

Name	**Sequence**	**Modification**	**Length**
T1	AGGCAGTTGAGACGAACATTCCTAAGTCTGAAATTTATC ACCCGCCATAGTAGACGTATCACC	n/a	63
T2-UN	ATGTTCGACATGCGAGGGTCCAATACCGACGATTACAGC TTGCTACACGATTCAGACTTAGGA	n/a	63
T3-UN	GGTGATAAAACGTGTAGCAAGCTGTAATCGACGGGAAGA GCATGCCCATCCACTACTATGGCG	n/a	63
T4-UN	CCTCGCATGACTCAACTGCCTGGTGATACGAGGATGGGC ATGCTCTTCCCGACGGTATTGGAC	n/a	63
T2-AT550	/5ATTO550N/ATGTTCGACATGCGAGGGTCCAATACCG ACGATTACAGCTTGCTACACGATTCAGACTTAGGA	AT550	63
T3-AF488	/5Alex488N/GGTGATAAAACGTGTAGCAAGCTGTAAT CGACGGGAAGAGCATGCCCATCCACTACTATGGCG	AF488	63
T4-AT633	/5ATTO633N/CCTCGCATGACTCAACTGCCTGGTGATA CGAGGATGGGCATGCTCTTCCCGACGGTATTGGAC	AT633	63

Table S3: Strands required for the assembly of each DNA structure.

Structure	Strand (stoichiometry)
Nanocrosshair	Core1 + Core2 + Core3 + NC-Core4 + AF488(4x) + AT550 (4x) + AT633 (4x)
Octacrosshair	Core1 + Core2 + Core3 + OC-Core4 + OC-Core5 + OC-Core6 + OC-Core7 + OC-Core8 + AF488(8x) + AT550 (8x) + AT633 (8x)
Tetrahedron	T1 + T2-AT550 + T3AF488 + T4 AT633

Section III: FRET analysis of the injected DNA structures

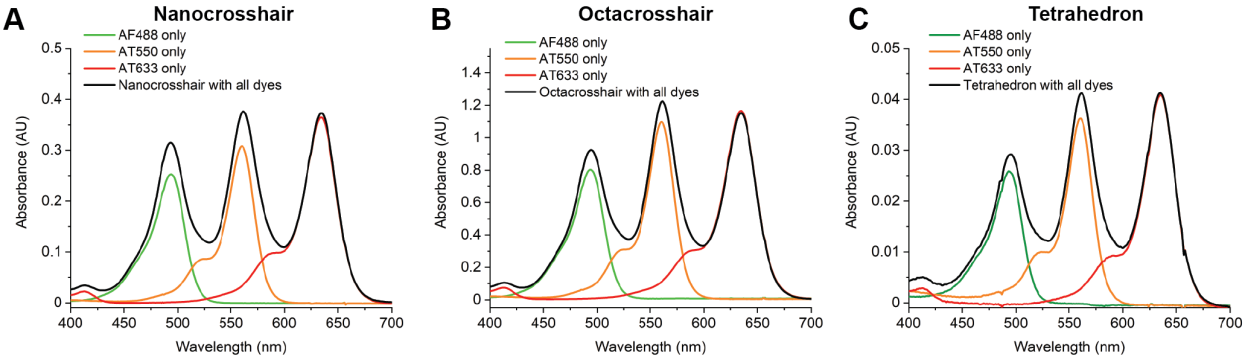

Figure S1: Steady-state absorbance in DNA of (A) nanocrosshair, (B) octacrosshair, and (C) tetrahedron and individual dye-oligos at 1 μM concentration of each structure.

Table S4: Spectral properties of the dyes in the structures.

	Ext Coeff @ $\lambda_{max\ abs}$ (M^{-1} cm^{-1})	Excitation max (λ nm)	Emission max (λ nm)	QY in crosshairs (ssDNA / full nano/octa)	QY in tetrahedron (ssDNA / full structure)
AF488 (D)	73,000	496	519	0.59 ± 0.06 / 0.87 ± 0.04	0.62 ± 0.05 / 0.74 ± 0.03
AT550 (R)	120,000	560	579	0.18 ± 0.02 / 0.19 ± 0.03	0.18 ± 0.03 / 0.20 ± 0.01
AT633 (A)	130,000	634	655	0.63 ± 0.03 / 0.75 ± 0.05	0.51 ± 0.04 / 0.63 ± 0.03

ssDNA = single stranded DNA

Table S5: Inter-dye distances (r_{DA}) within the DNA tetrahedron and crosshair structures based on observed steady-state FRET. The geometric r_{DA} predictions were estimated based on the architecture of the DNA structures, as illustrated in Figure S2. Experimentally determined r_{DA} were calculated from the steady state fluorescence spectra shown in Figure 1. The AF488-AT633 r_{DA} for the crosshairs was not determined as it is not significant as the structure is not capable of having just this FRET pair without the AT550 in the middle.

	AF488-AT550 (nm)	**AT550-AT633 (nm)**	**AF488-AT633 (nm)**
Tetrahedron			
Calculated R_0	6.2	5.2	5.3
Geometric DNA r_{DA} Predictions	6.1	5.0	4.8
Experimentally determined r_{DA}	8.0 ± 0.6	5.9 ± 0.9	8.9 ± 0.7
Crosshairs			
Calculated R_0	6.3	5.2	5.5
Geometric DNA r_{DA} Predictions	3.1	3.1	6.3
Experimentally determined r_{DA}	3.9 ± 0.4	4.4 ± 0.9	-

End-to-end FRET Efficiency (E_{ee}) is defined as the conditional probability that an exciton created at AF488 donor is transferred to AT633 acceptor molecule. The E_{ee} for the crosshairs was calculated to be 18 ± 7% and tetrahedron 7 ± 3%.

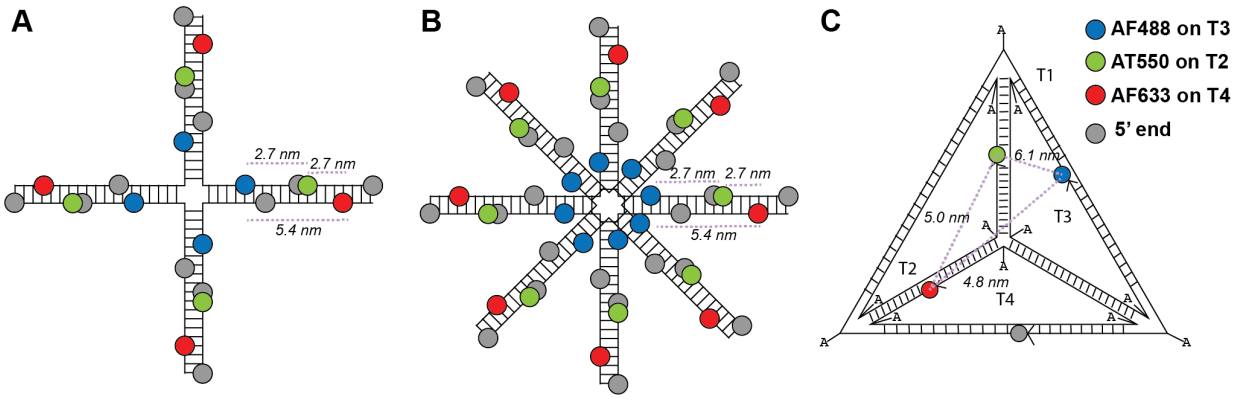

Figure S2: Two-dimensional representation of the architecture and predicted inter-dye distances in (A) nanocrosshair, (B) octacrosshair, and (C) tetrahedron. The inter-dye distances were estimated based on putative double stranded DNA dimensions of 0.34 nm per base.

Table S6: Number of cells injected per sample type for statistical analysis (n value).

Experiment (structure : cell type)	**Number of cells analyzed (n value)**
Nanocrosshair : COS cells	91
Tetrahedron : COS cells	85
Tetrahedron : Fibroblast cells	59
Tetrahedron : A549 cells	59
Tetrahedron : Astrocyte cells	52
Tetrahedron : HeLa cells	61
Nanocrosshair : HeLa cells	40

Image analysis.

Circular regions of interest (ROIs) of ~5 μm diameter were drawn in each cell cytosol and time-resolved fluorescence intensity was extracted from the fluorescence channels. From the fluorescence intensities, the following information was derived:

1. Total fluorescence in directly excited channels: Measurement of fluorescence in AF488 (excited at 488 nm), AT550 (excited at 561 nm), and AT633 (excited at 640 nm). **Figure S12** summarizes this result.
2. Total fluorescence in all channels excited at 488 nm: Measurement of fluorescence in AF488, AT550, and AT633 channels when excited at donor excitation wavelength 488 nm. This fluorescence represents FRET-triggered emission in each channel. **Figure S13** summarizes this result.
3. Normalized A/D ratio: Acceptor/Donor (both excited at 488 nm) ratio was calculated and normalized to set the ratio at t = 0 min to 1 (**Figures 3A-C, 4B-D, 5**) = $\frac{AT633\ Channel\ Fluorescence^{488\ nm}}{AF488\ Channel\ Fluorescence^{488\ nm}}$
4. Normalized A sensitization: Acceptor sensitization indicates the AT633 fluorescence due to FRET relative to the AT633 fluorescence upon direct excitation (at 640 nm) indicated by (**Figure 3D, 5**) = $\frac{AT633\ Channel\ Fluorescence^{488\ nm}}{AT633\ Channel\ Fluorescence^{641\ nm}}$

For each experiment, different channels were measured after excitation at the specified wavelengths (**Table S1**). **Figures S4-S11** show representative confocal images while **Figures S12** and **S13** represent the time-resolved total fluorescence in the relevant channels. Data acquisition was every 30 sec for 60 min. To facilitate quantitative analysis, imaging parameters (laser power, PMT gain, offset and threshold) were optimized for each DNA structure type since the number of fluorophores in each structure was different. Given that the DNA tetrahedron had low initial FRET, a single stranded DNA (ssDNA) control sample was also injected in COS cells and measured to validate that the confocal imaging settings were in fact sensitive to tetrahedron FRET readout. The ssDNA control sample (summarized in **Figures S11, S12F, S13F**) comprised of three orthogonal AF488-, AT550-, and AT633-labeled oligonucleotides were combined at 1 μM concentration to represent a fully deformed DNA tetrahedron control. As can be seen by comparing the A sensitization in tetrahedron (**Figure S13D**) *versus* the ssDNA control (**Figure S13F**) the

tetrahedron FRET is clearly resolved in the experimental setup. Moreover, free AT633-labeled oligo appears to drastically diminish from the cell in the ssDNA control sample (**Figure S12F**) whereas AT633 fluorescence in direct excited channel remains largely constant (**Figure S12D**).

To ensure that the presence of the microinjector needle did not cause leakage of the sample into the experimental petri dish and contribute to background signal, we compared the D and A fluorescence of injector background with DNA tetrahedron sample in COS cells (**Figure S15**). There was no unexpected background fluorescence due to the injector.

Table S7: Fluorescence measurements during confocal imaging.

Excitation wavelength → Channel name ↓	488 nm	560 nm	641 nm
AF488 (Green)	✕		
AT550 (Orange)	✕	✕	
AT633 (Red)	✕	✕	✕

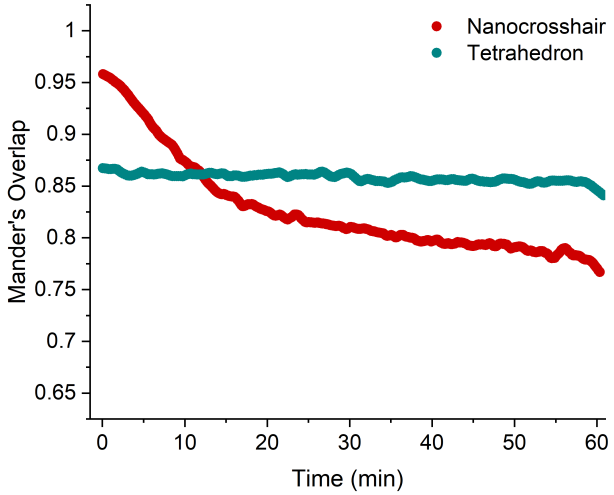

Figure S3: Colocalization coefficient change in COS-1 cytosol of AF488 and AT633 emission (at 488 nm excitation wavelength) observed in injected tetrahedron and nanocrosshair over time.

Using the ROIs drawn for FRET analysis, we determined the degree of colocalization (measured as the Mander's overlap[3] of the tetrahedron and nanocrosshair injected in COS-1 cells. The colocalization was measured between the donor AF488 fluorescence *versus* acceptor AT633 fluorescence when both are excited at donor excitation wavelength of 488 nm. Therefore, the coefficient (plotted in **Figure S3**) represents colocalization of FRET emissions. Both structures have high colocalization coefficients at t=0 min. Over time, the tetrahedron colocalization does not change while the nanocrosshair coefficient declines, indicating separation of fluorescence in the two channels.

Section IV: Representative confocal results for each sample at initial and end points

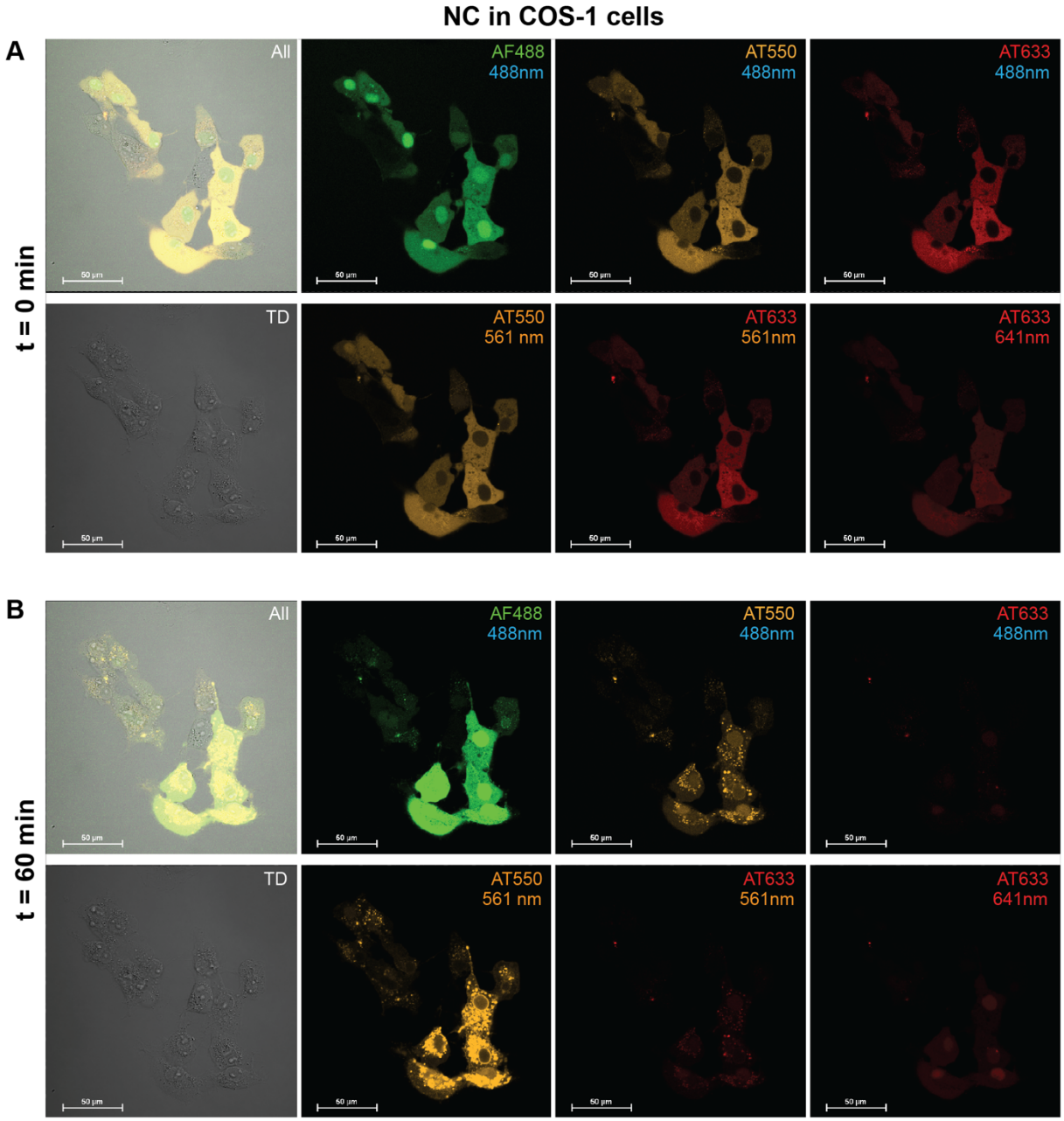

Figure S4: Representative confocal snapshots at initial and end timepoints of nanocrosshair injected in COS-1 cells. The top label (All, AF488, AT550, AT633) represents the channel while the bottom label (488 nm, 561 nm, 641 nm) represents the excitation wavelength in that channel.

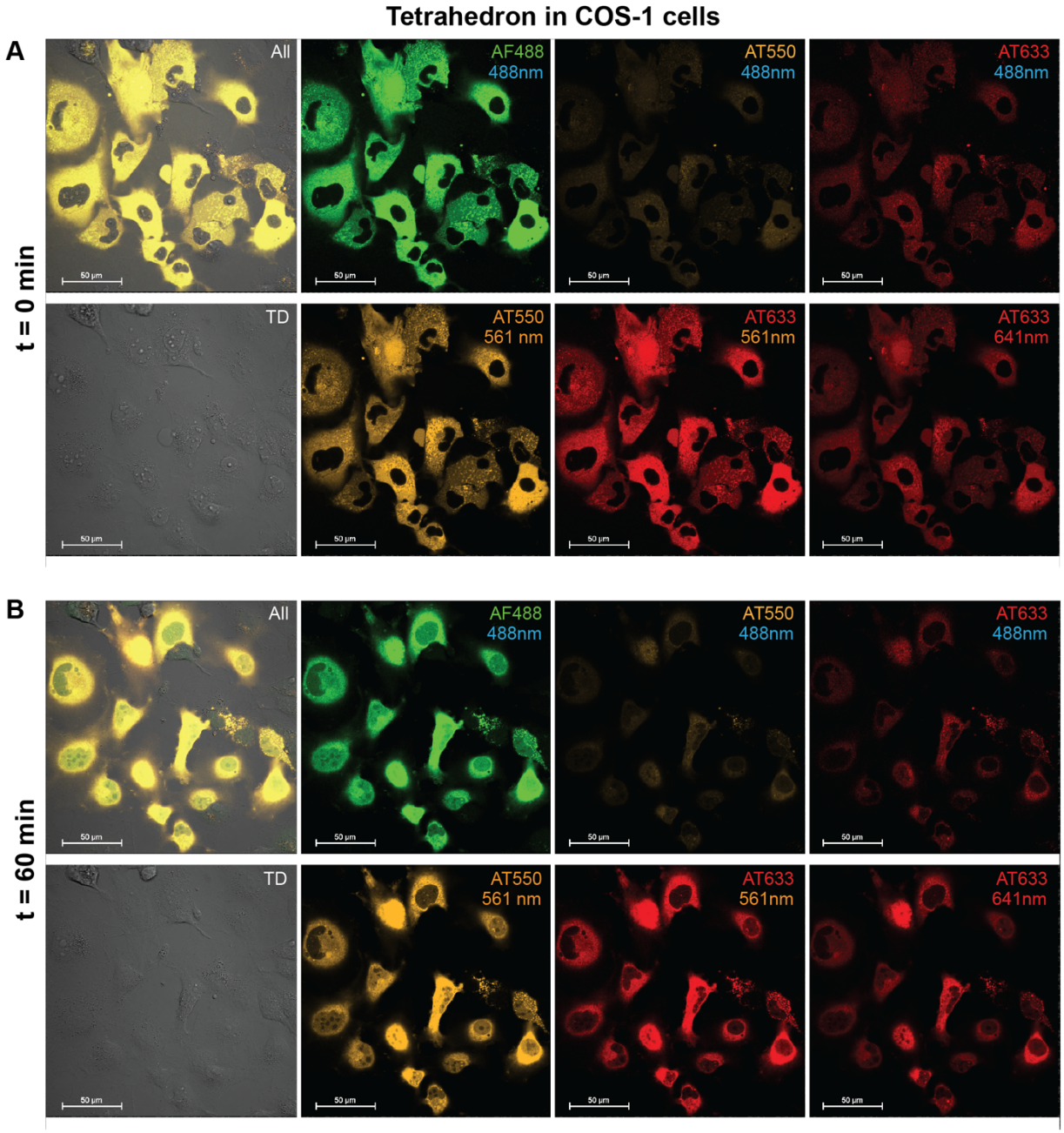

Figure S5: Representative confocal snapshots at initial and end timepoints of tetrahedron injected in COS-1 cells. The top label (All, AF488, AT550, AT633) represents the channel while the bottom label (488 nm, 561 nm, 641 nm) represents the excitation wavelength in that channel.

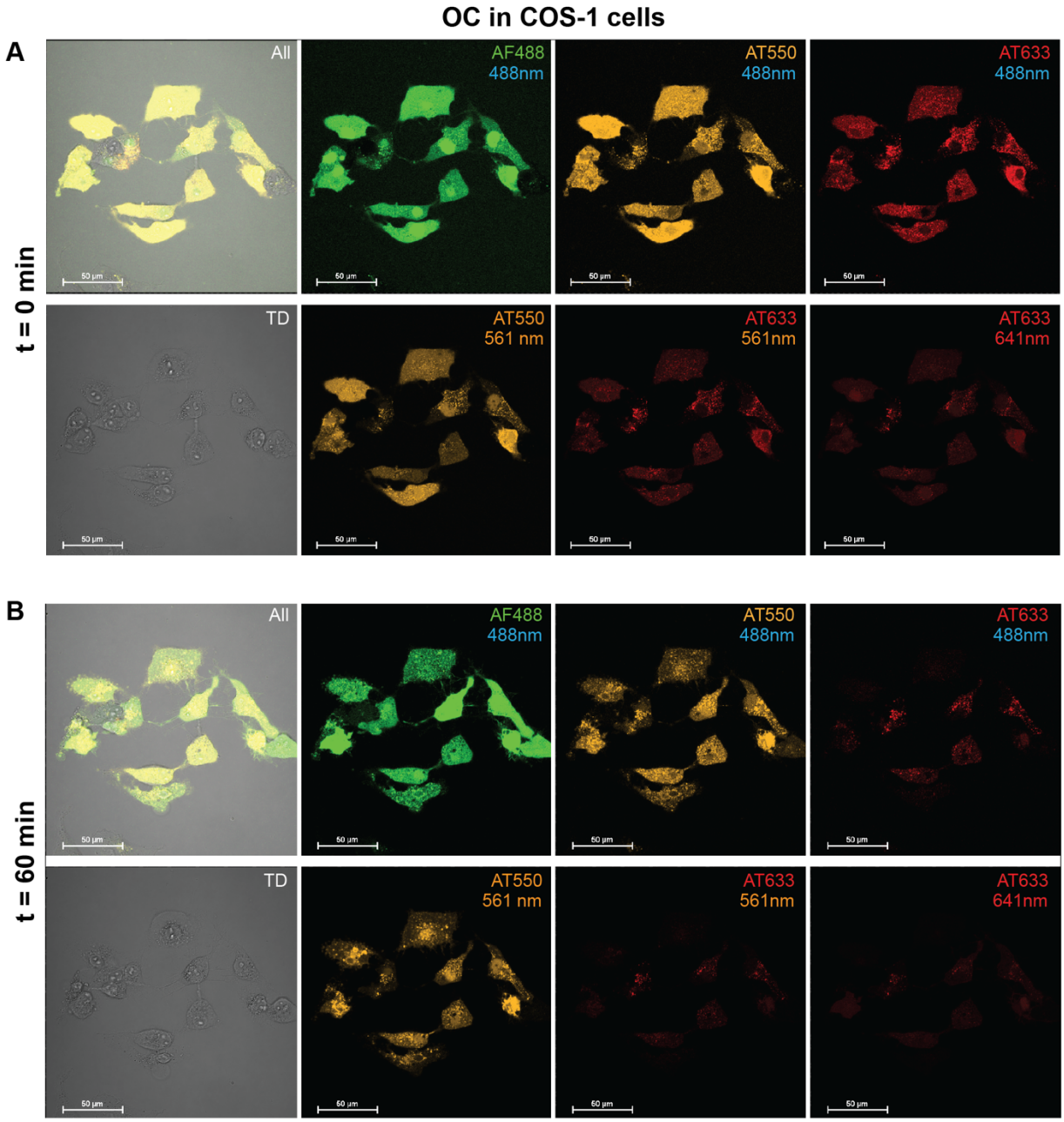

Figure S6: Representative confocal snapshots at initial and end timepoints of octacrosshair injected in COS-1 cells. The top label (All, AF488, AT550, AT633) represents the channel while the bottom label (488 nm, 561 nm, 641 nm) represents the excitation wavelength in that channel.

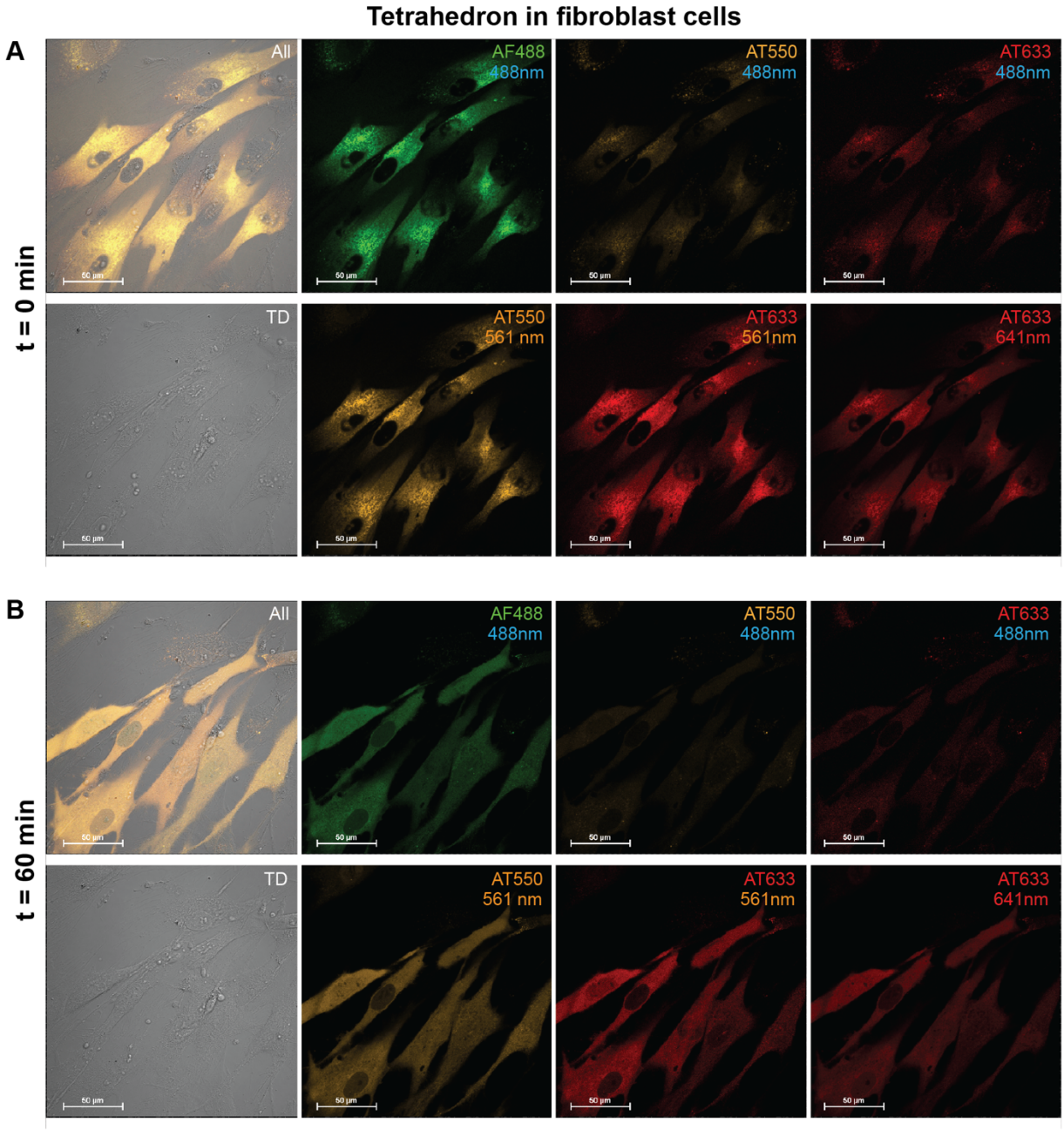

Figure S7: Representative confocal snapshots at initial and end timepoints of tetrahedron injected in fibroblast cells. The top label (All, AF488, AT550, AT633) represents the channel while the bottom label (488 nm, 561 nm, 641 nm) represents the excitation wavelength in that channel.

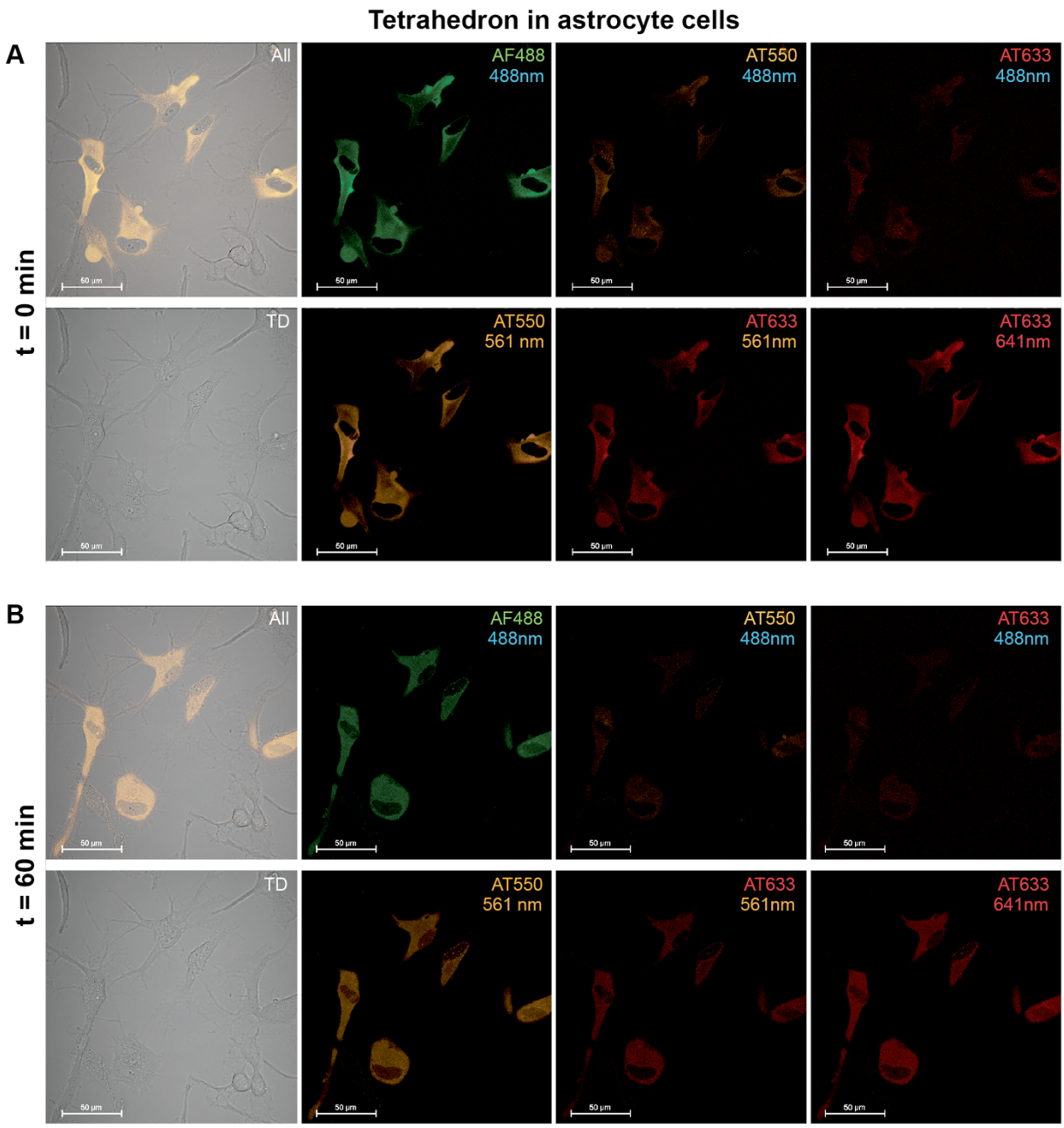

Figure S8: Representative confocal snapshots at initial and end timepoints of tetrahedron injected in human astrocyte cells. The top label (All, AF488, AT550, AT633) represents the channel while the bottom label (488 nm, 561 nm, 641 nm) represents the excitation wavelength in that channel.

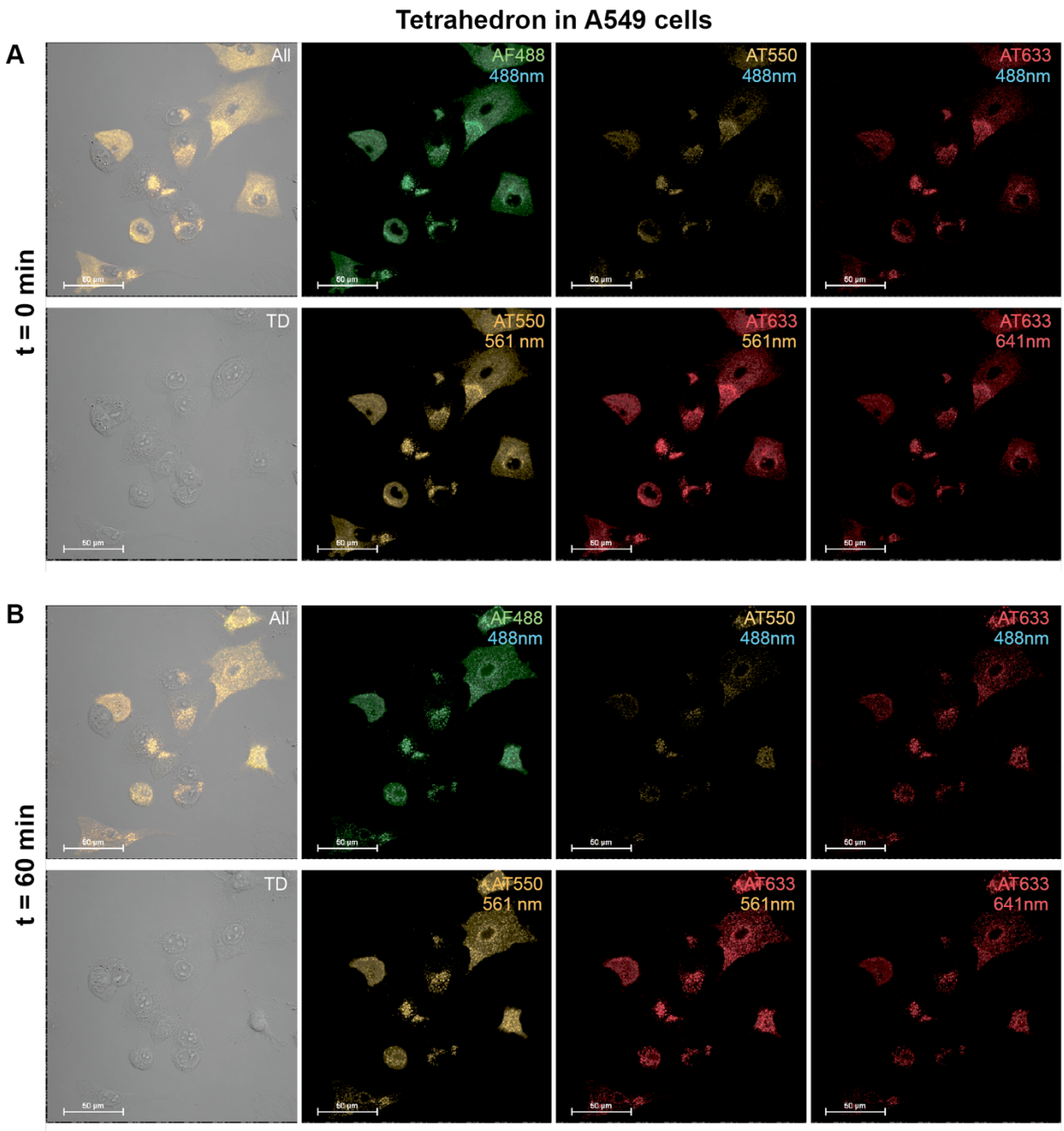

Figure S9: Representative confocal snapshots at initial and end timepoints of tetrahedron injected in A549 cells. The top label (All, AF488, AT550, AT633) represents the channel while the bottom label (488 nm, 561 nm, 641 nm) represents the excitation wavelength in that channel.

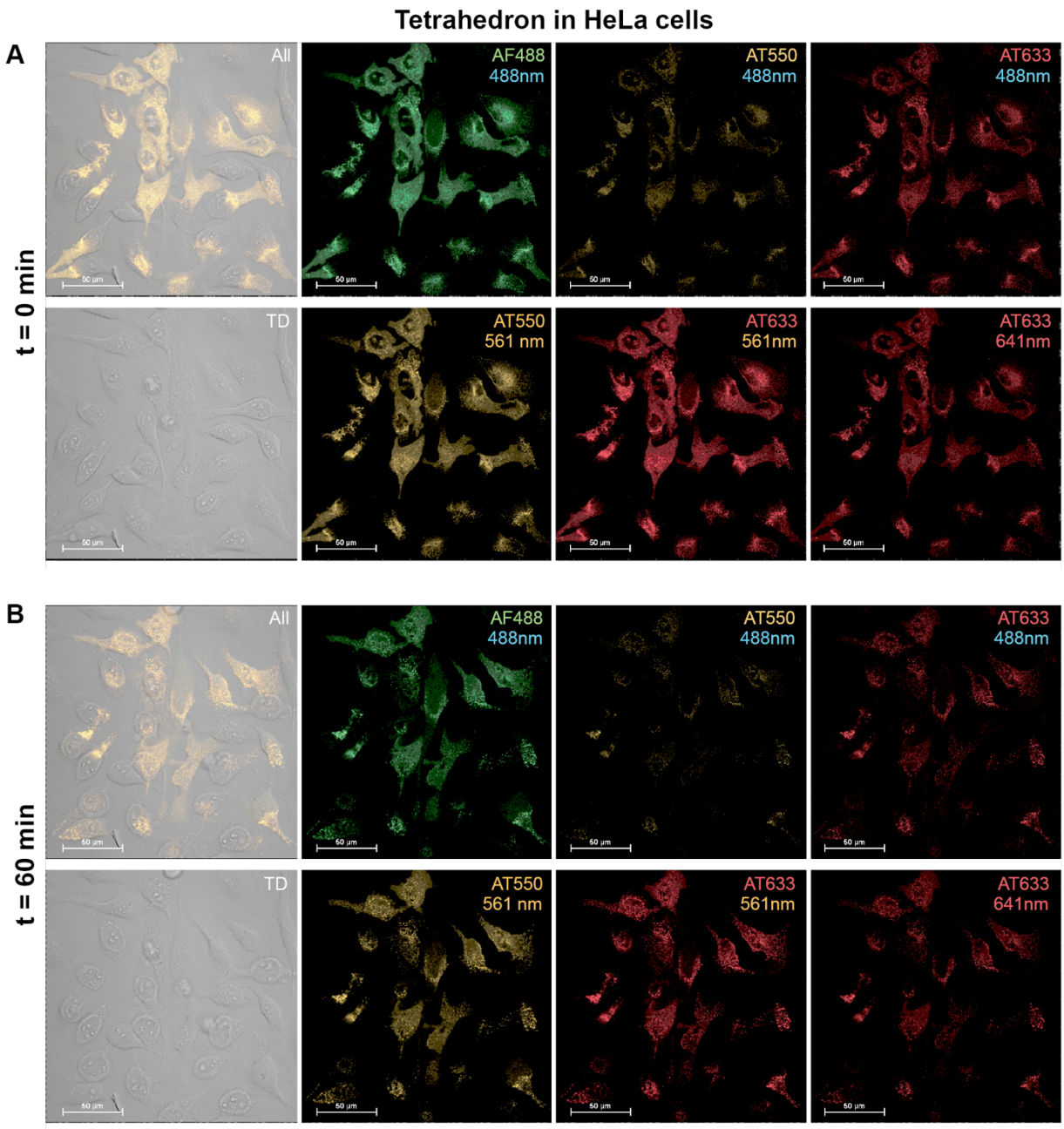

Figure S10: Representative confocal snapshots at initial and end timepoints of tetrahedron injected in HeLa cells. The top label (All, AF488, AT550, AT633) represents the channel while the bottom label (488 nm, 561 nm, 641 nm) represents the excitation wavelength in that channel.

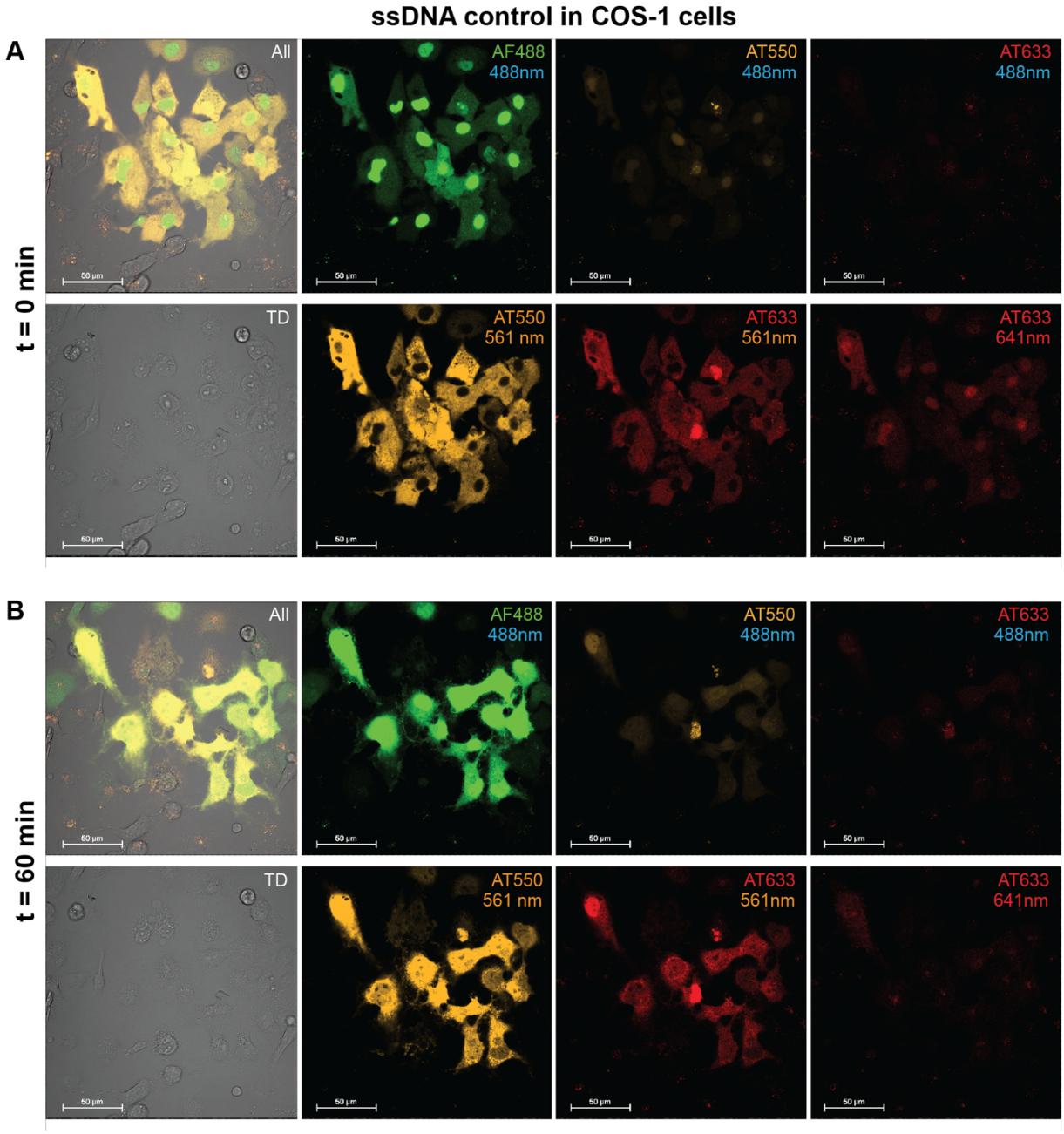

Figure S11: Representative confocal snapshots at initial and end timepoints of control ssDNA (mimicking 100% unformed tetrahedron) injected in COS-1 cells. The top label (All, AF488, AT550, AT633) represents the channel while the bottom label (488 nm, 561 nm, 641 nm) represents the excitation wavelength in that channel.

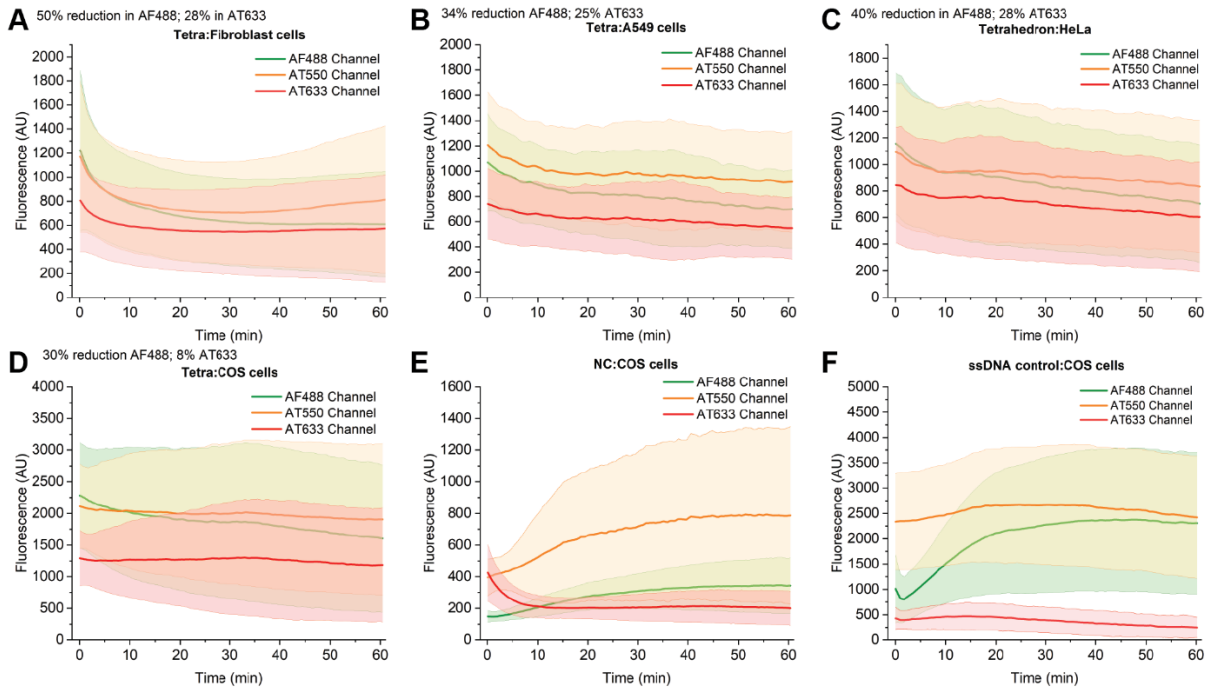

Figure S12: Total fluorescence in the three channels at direct excitation wavelength of the corresponding channel, namely – AF488 channel excited @ 488 nm, AT550 channel @ 561 nm, and AT633 channel @ 641 nm – in each injection sample type. These correspond to panels (ii), (vi), and (viii) in Figures S3-S9. Curves represent average fluorescence of ROIs that were identified for FRET analysis in this work and error band represents standard deviation from the mean.

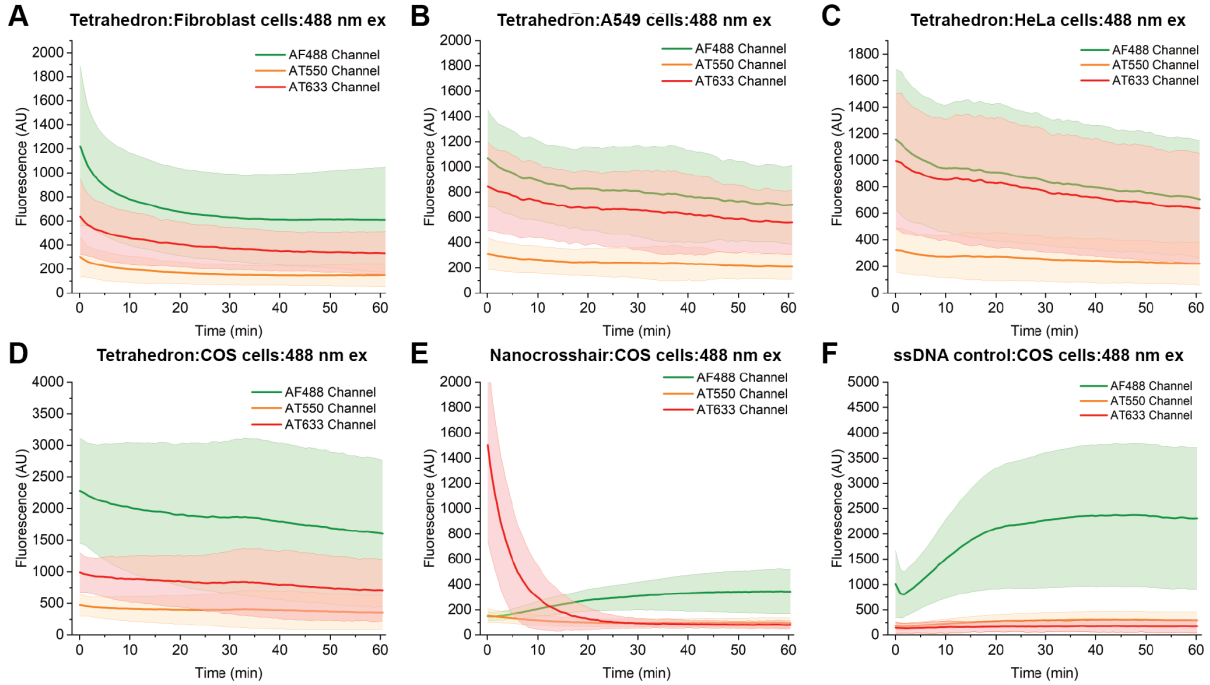

Figure S13: Total fluorescence in the three channels at 488 nm excitation wavelength, namely – AF488 channel excited @ 488 nm, AT550 channel @ 488 nm, and AT633 channel @ 488 nm – in each injection sample type. These correspond to panels (ii), (vi), and (viii) in Figures S3-S9. Curves represent average fluorescence of ROIs that were identified for FRET analysis in this work and error band represents standard deviation from the mean.

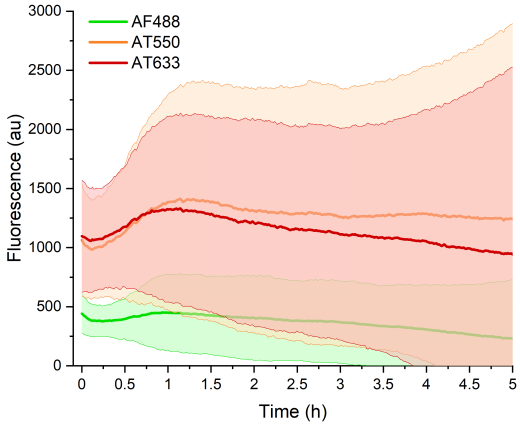

Figure S14: Total fluorescence in the three channels at 488 nm excitation wavelength namely – AF488 channel excited @ 488 nm, AT550 channel @ 488 nm, and AT633 channel @ 488 nm – in tetrahedron injected in COS-1 cells over 5 h. Curves represent average fluorescence of ROIs that were identified for FRET analysis in this work and error band represents standard deviation from the mean.

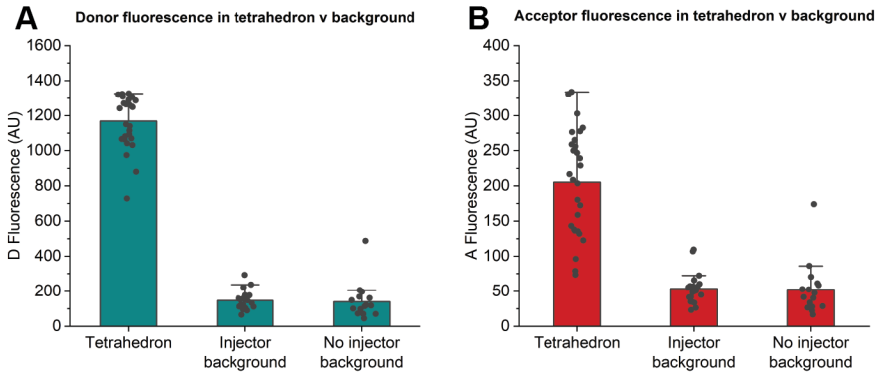

Figure S15: Background fluorescence due to microinjector during imaging in comparison to DNA tetrahedron signal.

References

1. Bamford, R. A.; Zhao, Z. Y.; Hotchin, N. A.; Styles, I. B.; Nash, G. B.; Tucker, J. H.; Bicknell, R. *PLoS One* **2014,** 9, (4), e95097.
2. Goetz, M.; Bubert, A.; Wang, G.; Chico-Calero, I.; Vazquez-Boland, J. A.; Beck, M.; Slaghuis, J.; Szalay, A. A.; Goebel, W. *Proc Natl Acad Sci U S A* **2001,** 98, (21), 12221-6.
3. Dunn, K. W.; Kamocka, M. M.; McDonald, J. H. *Am J Physiol Cell Physiol* **2011,** 300, (4), C723-42.